Precipitation Efficiency in the Tropical Deep Convective Regime

Xiaofan Li[1], *C.-H. Sui*[2], *K.-M.* Lau[2]

Submitted to the Journal of Meteorological Society of Japan

Popular Summary

Convection and associated precipitation plays an important role in regulating tropical climate. The development of the convection is related to many environmental and cloud factors such as environmental temperature and moisture distributions and transports and the exchanges among cloud contents. The processes associated with the development of the convection are so complicated that some simple parameters are needed for climate research. Precipitation efficiency is one such parameter. Generally, it measures the percentage of water condensed that precipitate out. We use a numerical model to simulate precipitation efficiency and to analyze the relationship between the precipitation efficiency and environmental temperature and between the precipitation efficiency and the intensity of the convection. We found that the precipitation is more efficient when heavy rainfall occurs over the warm region. The definitions of precipitation efficiency in this study could be applied to climate research.

[1]NOAA/NESDIS
[2]*NASA/Goddard Space Flight Center, Greenbelt, Maryland*

Abstract

Precipitation efficiency in the tropical deep convective regime is analyzed based on a 2-D cloud resolving simulation. The cloud resolving model is forced by the large-scale vertical velocity and zonal wind and large-scale horizontal advections derived from TOGA COARE for a 20-day period. Precipitation efficiency may be defined as a ratio of surface rain rate to sum of surface evaporation and moisture convergence (LSPE) or a ratio of surface rain rate to sum of condensation and deposition rates of supersaturated vapor (CMPE). Moisture budget shows that the atmosphere is moistened (dryed) when the LSPE is less (more) than 100 %. The LSPE could be larger than 100 % for strong convection. This indicates that the drying processes should be included in cumulus parameterization to avoid moisture bias.

Statistical analysis shows that the sum of the condensation and deposition rates is about 80 % of the sum of the surface evaporation rate and moisture convergence, which leads to proportional relation between the two efficiencies when both efficiencies are less than 100 %. The CMPE increases with increasing mass-weighted mean temperature and increasing surface rain rate. This suggests that precipitation is more efficient for warm environment and strong convection. Approximate balance of rates among the condensation, deposition, rain, and the raindrop evaporation is used to derive an analytical solution of the CMPE.

1. Introduction

Convection plays a most important role in regulating tropical climate. It redistributes atmospheric moisture, temperature, and momentum through cloud microphysical processes, latent heat release, and convective mixing respectively. Precipitation efficiency is an important physical parameter to measure interaction between convection and its atmospheric environment. The definition of the precipitation efficiency may vary. For the estimation of the surface rain rate with the large-scale variables in the cumulus parameterization (e.g., Kuo 1965, 1974), the precipitation efficiency is defined as a ratio of the surface rain rate to sum of surface evaporation and vertically-integrated horizontal and vertical specific humidity advections (moisture convergence). Consider a vertically-integrated moisture equation used in a 2-D cloud resolving model [e.g., Eq. (11b) in Li et al. 1999],

$$\frac{\partial [q_v]}{\partial t} = -P + E - [w^o \frac{\partial q_v}{\partial z}] - [u^o \frac{\partial q_v^o}{\partial x}]. \tag{1}$$

Here $[()] = \int_0^{z_T} \overline{\rho}() dz$, where z_T is the height of top model level. q_v is the specific humidity. u and w are the zonal wind and vertical velocity. P and E are the surface rain rate and surface evaporation rate respectively. Superscript o denotes imposed values from observations. The variables in (1) and the following equations are zonal mean.

After rearrangement, (1) becomes

$$\frac{\frac{\partial [q_v]}{\partial t}}{E - [w^o \frac{\partial q_v}{\partial z}] - [u^o \frac{\partial q_v^o}{\partial x}]} + \frac{P}{E - [w^o \frac{\partial q_v}{\partial z}] - [u^o \frac{\partial q_v^o}{\partial x}]} = 1. \tag{2}$$

The second term in the left hand side of (2) is the precipitation efficiency, which is referred to as large-scale precipitation efficiency (LSPE). The first term in the left hand side of (2) is a ratio of the local change of vertically-integrated specific humidity (precipitable water) to the sum of the surface evaporation and moisture convergence, which represents how much water vapor from vapor transport moistens the atmosphere. Eq. (2) set a constraint for the two quantities that the sum should be unity.

For the estimation of the surface rain rate with the cloud microphysics parameterization in the cloud resolving model (e.g., Li et al. 2001), the precipitation efficiency is

defined as a ratio of the surface rain rate to sum of vertically-integrated condensation and deposition rates, that is

$$\frac{P}{[P_{CND}] + [P_{DEP}] + [P_{SDEP}] + [P_{GDEP}]}. \tag{3}$$

Here P_{CND} is the growth rate of cloud water by the condensation of supersaturated vapor. P_{DEP} is the growth rate of cloud ice by the deposition of supersaturated vapor. P_{SDEP} and P_{GDEP} are the growth rates of snow and graupel by the vapor deposition respectively (see Li et al. 1999, 2001). This is referred to as cloud-microphysics precipitation efficiency (CMPE).

The central questions in this study are: what is the relationship between the LSPE and CMPE? what determines the precipitation efficiency? The model, forcing and experiment design are briefly described in the next section. The relation between the LSPE and CMPE is examined based on a 2-D cloud resolving simulation, and the cloud microphysics budget is used to derive the analytical solution of the CMPE in section 3. The summary will be given in section four.

2. The model, forcing and experiment design

The cloud resolving model was originally developed by Soong and Ogura (1980), Soong and Tao (1980), and Tao and Simpson (1993). The 2-D version of the model used by Sui et al. (1998) and modified by Li et al. (1999) is used in this study. The model includes cloud microphysics parameterization (Li et al. 2001). The details of the model can be referred to Li et al. (1999). The experiment analyzed in this study is conducted with the model forced by the zonally uniform vertical velocity, zonal wind, and horizontal advections, which are derived by Professor Minghua Zhang and his research group who used the 6-hourly TOGA COARE observations within the Intensive Flux Array (IFA) region. The calculations are based on the constrained variational method on column-integrated budgets of mass, heat, moisture, and momentum proposed by Zhang and Lin (1997). Hourly sea surface temperature at the Improved Meteorological (IMET) surface mooring buoy ($1.75^oS, 156^oE$) (Weller and Anderson 1996) is also imposed in the model. The model is integrated from

0400 19 December 1992 to 0400 9 January 1993 (local time). The horizontal domain is 768 km. A grid mesh of 1.5 km and a 12 second step are used in model integrations. Hourly simulation data are analyzed in the following discussions.

3. Results

Figure 1 shows the time evolution of the vertical distribution of the large-scale atmospheric vertical velocity and zonal wind during 19 December 1992-9 January 1993 that are imposed in the model. Within 19-25 December 1992, upward motion was dominant, indicating strong convection. From 26 December 1992-3 January 1993, downward motion became dominant, along with occasional upward motion, suggesting the dry phase. In the last few days, moderate upward motion occurred. The diurnal and two-day signals are also detected in Fig. 1a as indicated by Sui et al. (1997) and Takayabu et al. (1996) respectively. The large-scale westerly winds increase significantly in the lower- and mid-troposphere and reach their maximum of 20 ms^{-1} at 600 mb around 3 January 1993 (Fig. 1b). As mentioned previously, the model is also forced by the observed horizontal temperature and moisture advections (not shown), which have much smaller amplitudes than the vertical advections respectively. The comparison between simulation and observation of temperature and moisture is discussed in Li et al. (2001), and the causes of differences are intensively discussed in Li et al. (1999).

Fig. 2 shows the local change of the precipitable water versus surface rain rate. There is a tendency that the local change varies from the positive values to the The moisture convergence and surface evaporation support precipitation and moisten the environmental atmosphere in light rain regime (where the surface rain rate is smaller than 10 $mm\ day^{-1}$), whereas they are not enough to support precipitation and the environmental atmosphere loses moisture to feed convection and becomes drier in heavy rain regime (where the surface rain rate is larger than 30 $mm\ day^{-1}$). Thus, the moisture convergence and surface evaporation do not always mean that the atmosphere is moistened.

To further examine the relation between the local change of the precipitable water and surface rain rate, the ratio of the local change to the moisture sources [the first term

in the left hand side of (2) $\times$ 100 %] versus the LSPE [the second term in the left hand side of (2) $\times$ 100 %] is plotted in Fig. 3. The upper left square in Fig. 3 indicates the light rain regime where the atmosphere is always moistened by the moisture convergence and surface evaporation. Fig. 3 also shows that in the heavy rain regime (outside the upper left square) up to 60 % of moisture source for precipitation come from the drying processes of the environmental atmosphere. This suggests that the drying effects be included in cumulus parameterization schemes to avoid moisture bias. Note the strictly linear relation between the two quantities which is constrained by (2).

Cloud formation links the precipitation and environmental moisture buildup. Thus, the condensation and deposition are the key processes during the cloud development. Li et al. (2001) showed that $[P_{CND}]$ and $[P_{DEP}]$ are much larger than $[P_{SDEP}]$ and $[P_{GDEP}]$. The sum of $[P_{CND}]$ and $[P_{DEP}]$ versus the sum of the surface evaporation and moisture convergence is plotted in Fig. 4. There is a statistical linear relation between the two sums. The linear correlation coefficient is 0.68, which exceeds 99 % confidence level. This statistical linear relation indicates that about 80 % of the sum of the moisture convergence and surface evaporation is used to be condensed and deposited. The statistical straight line approximately divides this scattering plot into the two different regimes. The moisture convergence and surface evaporation fully support the condensation and deposition in the light rain regime below this line, whereas the environmental atmosphere undergoes drying in the heavy rain regime above this line.

If $y = [P_{CND}] + [P_{DEP}]$, and $x = E - [w^o \frac{\partial q_v}{\partial z}] - [u^o \frac{\partial q_v^o}{\partial x}]$, the equation that governs this statistical line is expressed as

$$y = 4.05 + 0.84x. \tag{4}$$

Substituting (4) into (3), we have the approximate relation between the CMPE and LSPE.

$$CMPE = \frac{P}{y} = \frac{P}{4.05 + 0.84x} \simeq 1.19\frac{P}{x} = 1.19 LSPE. \tag{5}$$

Note that (5) is valid for large x. (5) simply states that the CMPE and LSPE are proportional. This can be seen in Fig. 5. However, (5) is only valid when both efficiencies are

less than 100 % since the CMPE is less than 100 %. Fig. 5 also shows that the CMPE is nearly statistically constant when the LSPE exceeds 100 %.

Li et al. (2001) showed that $[P_{CND}] + [P_{DEP}] = P + [P_{REVP}]$, where P_{REVP} is the evaporation rate of raindrop. Thus, the analytic expression of the CMPE is expressed by

$$CMPE = \frac{P}{[P_{CND}] + P_{DEP}]} = 1 - \frac{[P_{REVP}]}{[P_{CND}] + P_{DEP}]}. \tag{6}$$

Here

$$P_{CND} + P_{DEP} = \frac{1}{\Delta t} \frac{q_v - (q_{ws} + q_{is})}{1 + (\frac{A_1 q_c q_{ws}}{q_c + q_i} + \frac{A_2 q_i q_{is}}{q_c + q_i})(\frac{L_v}{c_p}\frac{T - T_{00}}{T_0 - T_{00}} + \frac{L_s}{c_p}\frac{T_0 - T}{T_0 - T_{00}})}, \tag{6a}$$

where $q_{ws} = \frac{B}{p} e^{(D_1 - \frac{E_1}{T - F_1})}$ and $q_{is} = \frac{B}{p} e^{(D_2 - \frac{E_2}{T - F_2})}$ are the saturation mixing ratio for water and ice respectively; q_c and q_i are mixing ratios of cloud water and ice respectively; L_v and L_s are heat coefficients due to condensation and deposition respectively; c_p is the specific heat of dry air at constant pressure; $A_1 = \frac{E_1}{(T - F_1)^2}$; $A_2 = \frac{E_2}{(T - F_2)^2}$; $B = 3.799052$; $D_1 = 17.26939$; $D_2 = 21.87456$; $E_1 = 4098.026$; $E_2 = 5807.695$; $F_1 = 35.86$; $F_2 = 7.66$; $T_0 = 0^o C$; $T_{00} = -35^o C$. In (6a), the schemes of Tao et al. (1989) are used.

$$P_{REVP} = \frac{2\pi N_{0R}(S - 1)}{\rho(A' + B')}[\frac{0.78}{\lambda_R^2} + 0.31(\frac{a'\rho}{\mu})^{\frac{1}{2}}(\frac{\rho_0}{\rho})^{\frac{1}{4}}\frac{\Gamma(3)}{\lambda_R^3}], \tag{6b}$$

where $S(= \frac{q_v}{q_{ws}})$ is saturated ratio with respect to water; $\pi = (\frac{p}{p_o})^{\kappa}$, $\kappa = \frac{R}{c_p}$, R is the gas constant; $N_{0R}(= 8 \times 10^6\ m^{-4})$ is the intercept value in raindrop size distribution; $a'(= 3 \times 10^3\ s^{-1})$ is the constant in linear fallspeed relation for rain; $\lambda_R[= (\frac{\pi \rho_L N_{0R}}{\rho q_r})^{\frac{1}{4}}]$ is the slope of raindrop size distribution; $\rho_L(= 10^3 kgm^{-3})$ is the density of raindrop; ρ is the air density which is a function of height only; ρ_o is ρ at surface; $A' = \frac{L_v}{K_a T}(\frac{L_v M_w}{RT} - 1)$; $B' = \frac{RT}{\chi M_w e_{ws}}$ (Pruppacher and Klett 1978); Γ is the Gamma function; $\mu(= 1.718 \times 10^{-5}\ kgm^{-1}s^{-1})$ is the dynamic viscosity of air. In (6b), the scheme of Rutledge and Hobbs (1983) is used.

Eq. (6) states that the sum of the CMPE and raindrop evaporation efficiency (that is defined by a ratio of evaporation rate of raindrop to the sum of the condensation and deposition rates) should be unity. A large CMPE means a small raindrop evaporation

efficiency, and vice versa. Li et al. (2001) showed that $P_{CND} + P_{DEP}$ in (6a) is dominated by $q_v - (q_{ws} + q_{is})$, and the second term of the right hand side in (6b) is much larger than the first term. Thus, The CMPE is functions of the falling speed of rain, the covariance between $S-1$ and q_r, and difference between the specific humidity minus the sum saturated mixing ratios for water and ice.

Since the CMPE is closely related to the environmental thermodynamic parameters and cloud parameters, the relationships between the CMPE and mass-weighted mean temperature (Fig. 6), and between the CMPE and SST (Fig. 7), and between the CMPE and surface rain rate (Fig. 8) are analyzed. The mean CMPE increases and the range of the CMPE variation decreases with increasing mass-weighted mean temperature, in particular, from -11^oC to -8^oC. This indicates that the precipitation is more efficient when the environmental atmosphere is warmer. The mean CMPE decreases with increasing SST from 28^oC to 29^oC, and increases from 29^oC to 30^oC. The nearly linear relation between the mass-weighted mean temperature and SST (not shown) causes the similar CMPE variations with the mass-weighted mean temperature and SST for warmer mass-weighted mean temperature (larger than -11^oC) and warmer SST (larger than 29^oC). The variations of the CMPE in the colder mass-weighted mean temperature (less than -11^oC) are different from those in the colder SST (less than 29^oC). This is due to the fact that there is no significant relationship between the mass-weighted mean temperature and SST for the colder mass-weighted mean temperature and colder SST (not shown). The temperature is more determined by the residual between the vertical temperature advection and condensational heating (Li et al. 2001) than by the SST in the cloud resolving model since the large-scale vertical velocity is imposed. The mean CMPE increases but the range of the CMPE variation decreases dramatically with increasing surface rain rate. The CMPE varies from 20 % to 90 % in the light rain regime, and from 60 % to 80 % in the heavy rain regime. For the heaviest rain (the surface rain rate is larger than 40 $mm\ day^{-1}$), the CMPE is about 78 %. Since the life cycle of the simulated convection is about 9 days (Li et al. 2000), the above calculations are repeated for 6 hourly data, and the results are generally similar to the corresponding results for hourly data.

4. Summary

Precipitation efficiency in the tropical deep convective regime is investigated by analyzing a 2-D cloud resolving simulation. The cloud resolving model is integrated for 20 days with the forcing of large-scale vertical velocity and zonal wind, as well as the large-scale horizontal advections derived from TOGA COARE data. Analysis of moisture budget shows that the atmosphere is moistened when the convection is weak, and it is dryed when the convection is strong. Surface evaporation and moisture convergence are not enough for development of strong convection so that atmospheric moisture is extracted to support heavy precipitation. If large-scale precipitation efficiency is defined as the ratio of the surface rain rate to the sum of the surface evaporation and moisture convergence, it can exceeds 100 % for the strong convection as shown in many cases during the integration. Thus, the drying processes of environmental atmosphere associated with the strong convection should be included in the cumulus parameterization to avoid moisture bias.

Statistical analysis shows that the sum of the condensation and deposition rates of supersaturated vapor are approximately 80 % of the sum of the surface evaporation and moisture convergence. If cloud-microphysics precipitation efficiency is defined as the ratio of the surface rain rate to the sum of the condensation and deposition rates, the ratio of cloud-microphysics precipitation efficiency to large-scale precipitation efficiency is about 1.19 when both efficiencies are less than 100 %. The cloud-microphysics precipitation is roughly a constant when the large-scale precipitation efficiency exceeds 100 %.

The cloud-microphysics precipitation efficiency depends on the environmental thermodynamics and cloud microphysics. The efficiency increases with increasing mass-weighted mean temperature and surface rain rate. This suggests that the precipitation be more efficient in heavy rain regime under warm environmental condition. Since the condensation and deposition rates of supersaturated vapor balances rain rate and the evaporation rate of raindrop in the tropical deep convective regime (Li et al. 2001), the analytical solution of cloud-microphysics precipitation efficiency is derived. The cloud-microphysics precipitation efficiency depends on the falling speed of raindrop, the difference between specific

humidity and the saturated specific humidity, and the covariance between the specific humidity difference and mixing ratio of raindrop. and the saturated specific humidity.

Acknowledgments. Authors thank Prof. M. Zhang at the State University of New York at Stony Brook for allowing us to use his TOGA COARE forcing data. This research is supported under the TRMM projects of NASA's Mission to Planet Earth Office.

References

Kuo, H. L., 1965: On formation and intensification of tropical cyclones through latent heat release by cumulus convection. *J. Atmos. Sci.*, **22**, 40-63.

Kuo, H. L., 1974: Further studies of the parameterization of the influence of cumulus convection on large-scale flow. *J. Atmos. Sci.*, **31**, 1232-1240.

Li, X., C.-H. Sui, K.-M. Lau, and M.-D. Chou, 1999: Large-scale forcing and cloud-radiation interaction in the tropical deep convective regime. *J. Atmos. Sci.*, **56**, 3028-3042.

Li, X., C.-H. Sui, and K.-M. Lau, 2000: Interactions between tropical convection and its environment: An energetics analysis of a 2-D cloud resolving simulation. *J. Atmos. Sci.*, (Revised).

Li, X., C.-H. Sui, and K.-M. Lau, 2001: CLoud microphysics budget in the tropical deep convective regime. *J. Meteor. Soc. Japan*, (Submitted).

Pruppacher, H. R., and J. O. Klett, 1978: Microphysics of clouds and precipitation. Reidel, 714pp.

Rutledge, S. A., and R. V. Hobbs, 1983: The mesoscale and microscale structure and organization of clouds and precipitation in midlatitude cyclones. Part VIII: A model for the "sender-feeder" process in warm-frontal rainbands. *J. Atmos. Sci.*, **40**, 1185-1206.

Soong, S. T., and Y. Ogura, 1980: Response of tradewind cumuli to large-scale processes. *J. Atmos. Sci.*, **37**, 2035-2050.

Soong, S. T., and W. K. Tao, 1980: Response of deep tropical cumulus clouds to mesoscale processes. *J. Atmos. Sci.*, **37**, 2016-2034.

Sui, C.-H., K.-M. Lau, Y. Takayabu, and D. Short, 1997: Diurnal variations in tropical oceanic cumulus ensemble during TOGA COARE. *J. Atmos. Sci.*, **54** 639-655.

Sui, C.-H., X. Li, and K.-M. Lau, 1998: Radiative-convective processes in simulated diurnal variations of tropical oceanic convection. *J. Atmos. Sci.*, **55**, 2345-2359.

Takayabu, Y. N., K.-M. Lau, and C.-H. Sui, 1996: Observation of a quasi-2-day wave during TOGA COARE. *Mon. Wea. Rev.*, **124**, 1892-1913.

Tao, W.-K., and J. Simpson, 1993: The Goddard Cumulus Ensemble model. Part I: Model description. *Terr. Atmos. Oceanic Sci.*, **4**, 35-72.

Tao, W.-K., J. Simpson, and M. McCumber, 1989: An ice-water saturation adjustment. *Mon. Wea. Rev.*, **117**, 231-235.

Weller, R. A., and S. P. Anderson, 1996: Surface meteorology and air-sea fluxes in the western equatorial Pacific warm pool during TOGA COARE. *J. Climate*, **9**, 1959-1990.

Zhang, M. H., and J. L. Lin, 1997: Constrained variational analysis of sounding data based on column-integrated budgets of mass, heat, moisture, and momentum: Approach and application to ARM measurements. *J. Atmos. Sci.*, **54**, 1503-1524.

Figure Captions

Fig. 1 Time evolution of (a) vertical velocity ($mb\ hour^{-1}$), and (b) zonal wind (ms^{-1}) taken from the TOGA COARE for a 20-day period. Downward motion in (a) and westerly wind in (b) are shaded.

Fig. 2 Local change of precipitable water versus surface rain rate. Unit is $mm\ day^{-1}$.

Fig. 3 Ratio of local change of precipitable water to sum of surface evaporation and moisture convergence versus large-scale precipitation efficiency. Unit is %.

Fig. 4 Sum of condensation and deposition rates versus sum of surface evaporation and vertically-integrated horizontal and vertical moisture advections. Unit is $mm\ day^{-1}$.

Fig. 5 Cloud-scale precipitation efficiency versus large-scale precipitation efficiency. Unit is %.

Fig. 6 Cloud-scale precipitation efficiency (%) versus mass-weighted mean temperature (^oC).

Fig. 7 Cloud-scale precipitation efficiency (%) versus SST (oC).

Fig. 8 Cloud-scale precipitation efficiency (%) versus surface rain rate ($mm\ day^{-1}$).

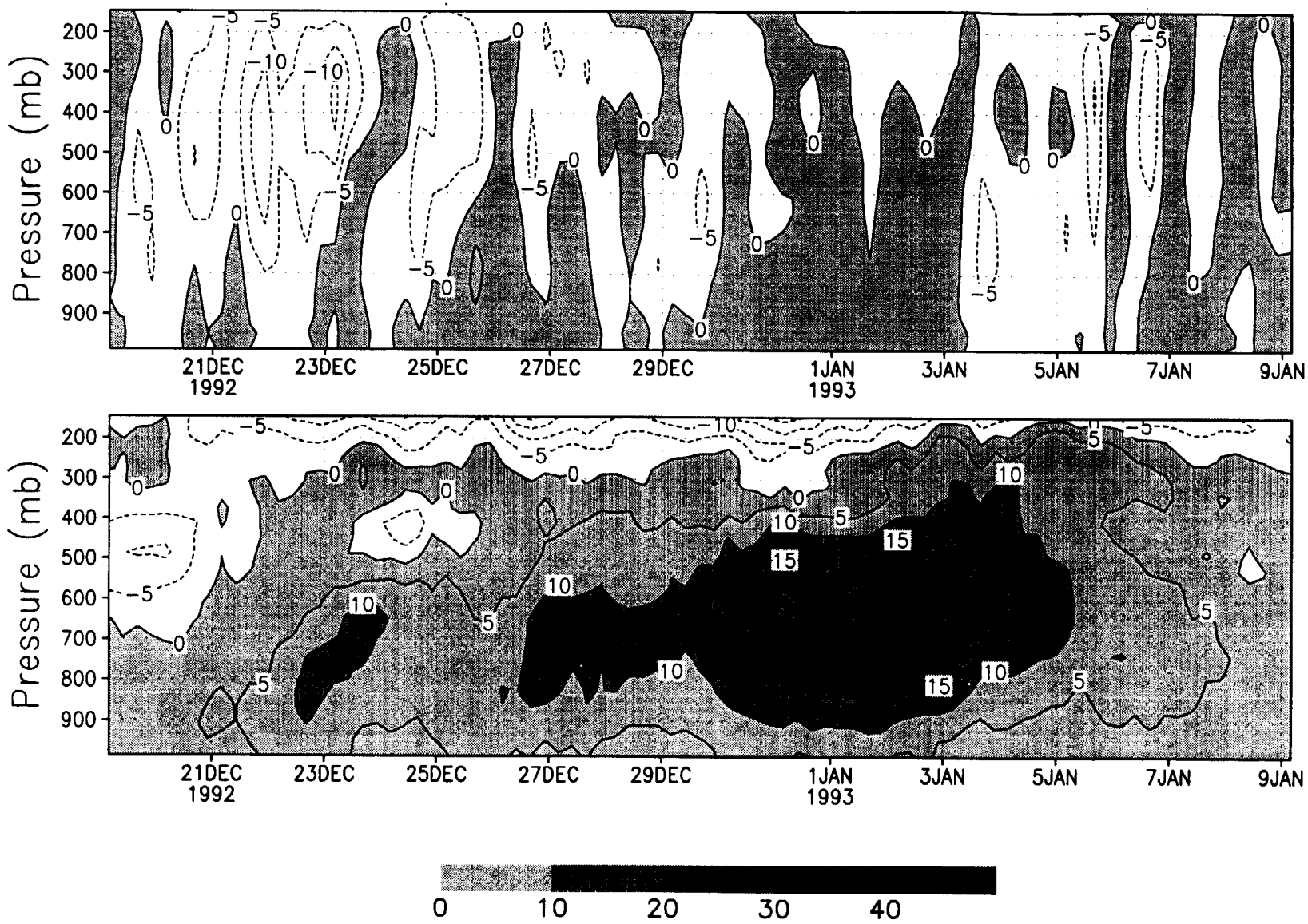
Pressure (mb)
200
300
400
500
600
700
800
900
21DEC
1992
23DEC
25DEC
27DEC
29DEC
1JAN
1993
3JAN
5JAN
7JAN
9JAN
0
10
20
30
40

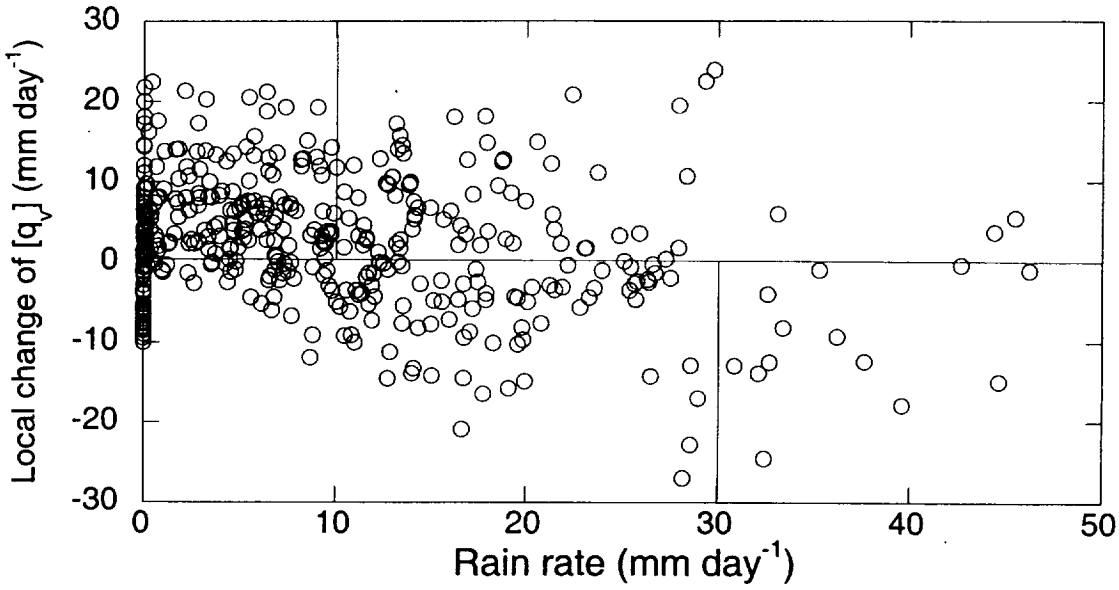
30
20
10
0
-10
-20
-30
0
10
20
30
40
50
Local change of [q_v] (mm day^{-1})
Rain rate (mm day^{-1})

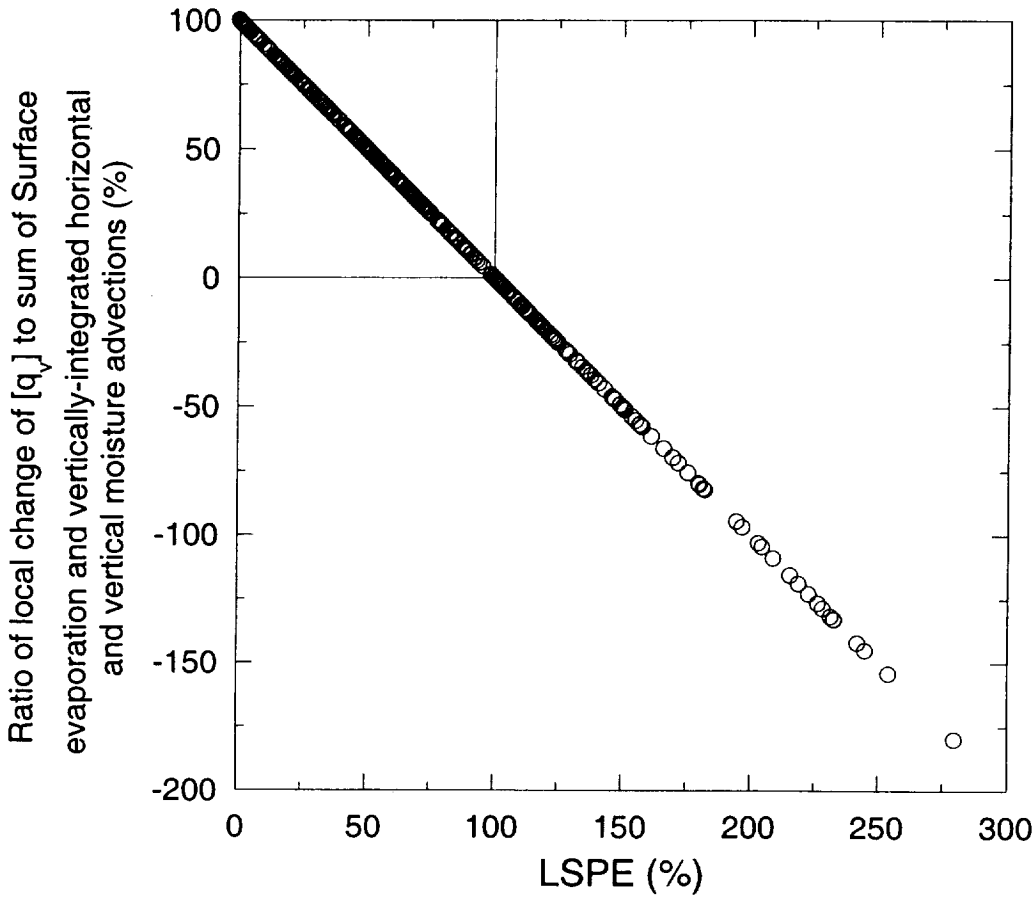
Ratio of local change of [q_v] to sum of Surface evaporation and vertically-integrated horizontal and vertical moisture advections (%)
100
50
0
-50
-100
-150
-200
0
50
100
150
200
250
300
LSPE (%)

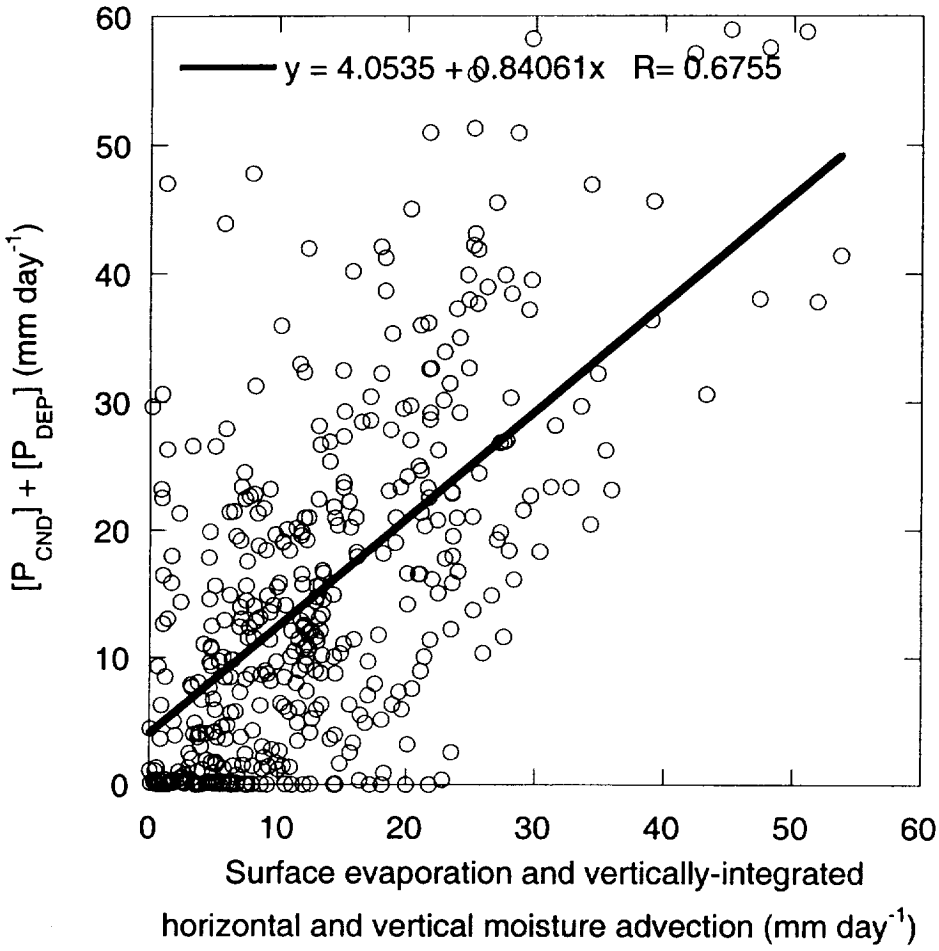
y = 4.0535 + 0.84061x R= 0.6755
[P_CND] + [P_DEP] (mm day^-1)
Surface evaporation and vertically-integrated
horizontal and vertical moisture advection (mm day^-1)
0
10
20
30
40
50
60

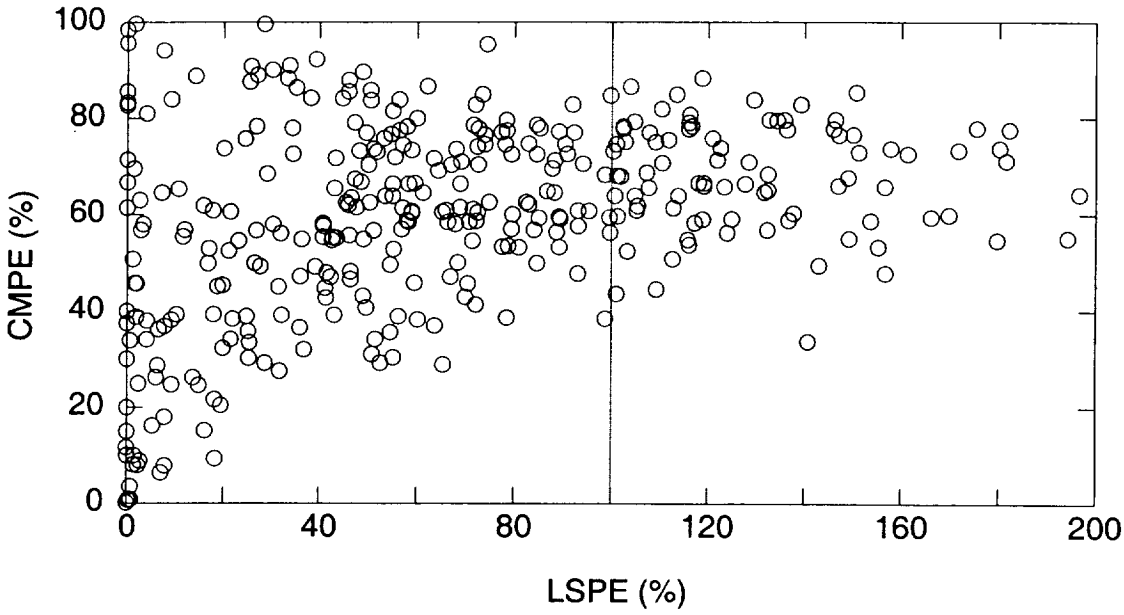
100
80
60
40
20
0
CMPE (%)
0
40
80
120
160
200
LSPE (%)

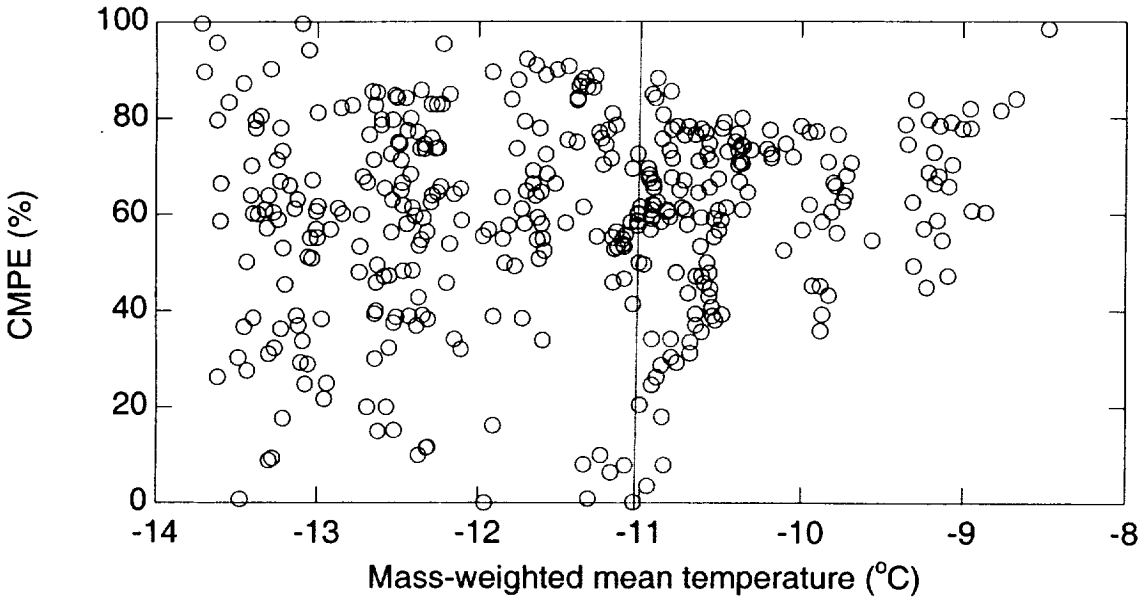
100
80
60
40
20
0
CMPE (%)
-14
-13
-12
-11
-10
-9
-8
Mass-weighted mean temperature (°C)

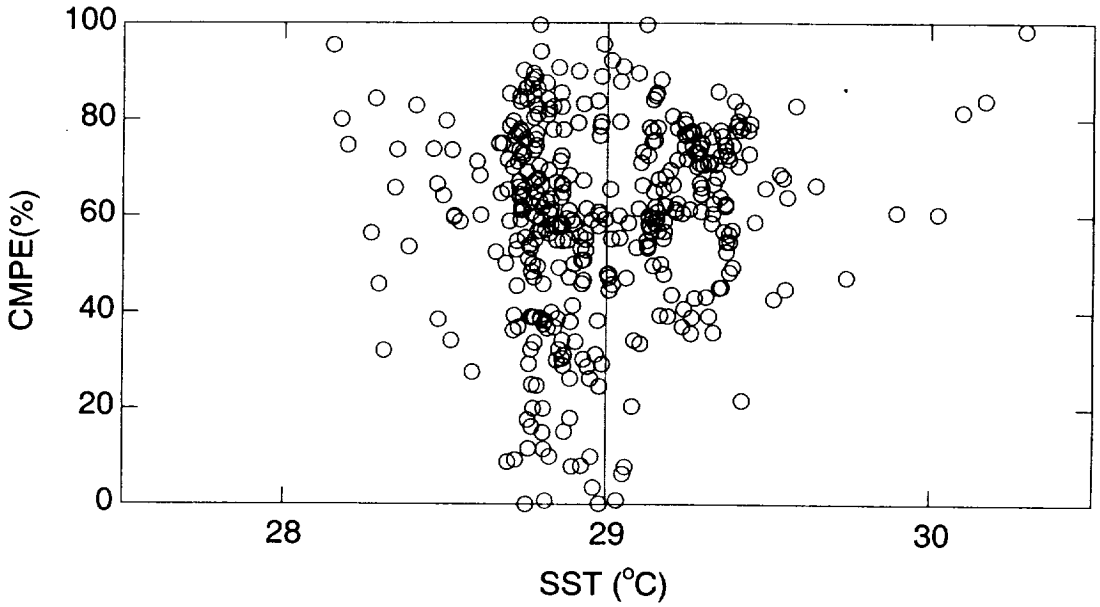
100
80
60
40
20
0
CMPE(%)
28
29
30
SST (°C)

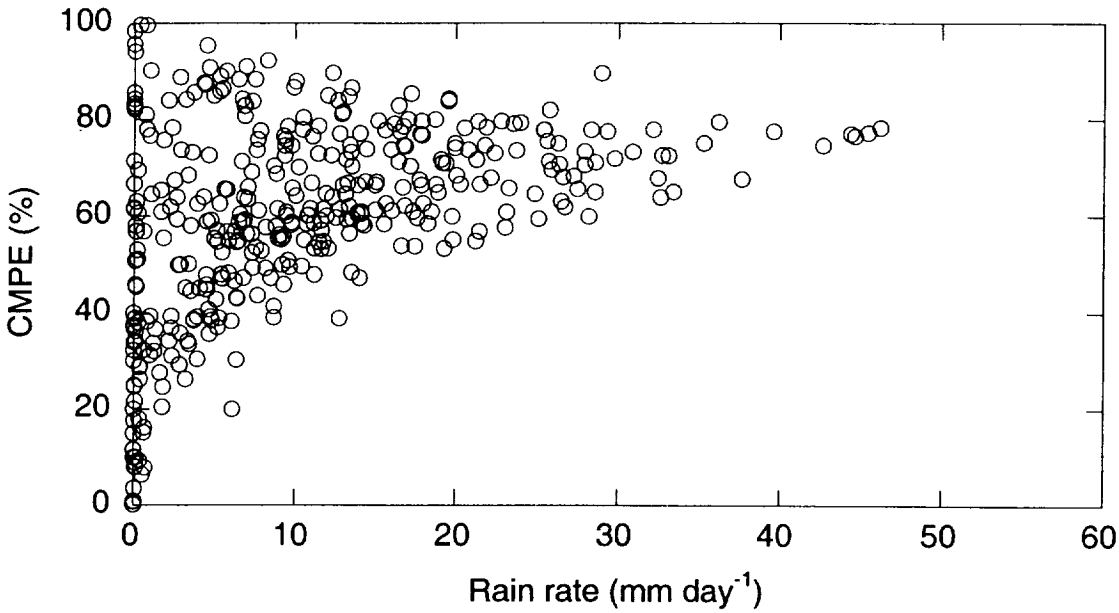
100
80
60
40
20
0
CMPE (%)
0
10
20
30
40
50
60
Rain rate (mm day-1)

Precipitation Efficiency in the Tropical Deep Convective Regime

Xiaofan Li[1], C.-H. Sui[2], K.-M. Lau

NASA/Goddard Space Flight Center, Greenbelt, Maryland

June, 2001

[1]Current affiliation: NOAA/NESDIS/Office of Research and Applications, Camps Spring, MD

[2]Corresponding author address: Dr. C.-H. Sui, NASA/GSFC, Code 913, Greenbelt, MD 20771 Email:sui@climate.gsfc.nasa.gov